

# Liquid-Infused Silicone As a Biofouling-Free Medical Material

Noah MacCallum,<sup>†</sup> Caitlin Howell,<sup>†,‡</sup> Philseok Kim,<sup>†</sup> Derek Sun,<sup>†</sup> Ronn Friedlander,<sup>‡</sup> Jonathan Ranisau,<sup>†</sup> Onye Ahanotu,<sup>†</sup> Jennifer J. Lin,<sup>†</sup> Alex Vena,<sup>†</sup> Benjamin Hatton,<sup>†</sup> Tak-Sing Wong,<sup>†</sup> and Joanna Aizenberg<sup>\*,†,‡,§</sup>

<sup>†</sup>Wyss Institute for Biologically Inspired Engineering, <sup>‡</sup>School of Engineering and Applied Sciences, and <sup>§</sup>Department of Chemistry and Chemical Biology, Harvard University, Cambridge, Massachusetts, United States

## Supporting Information

**ABSTRACT:** There is a dire need for infection prevention strategies that do not require the use of antibiotics, which exacerbate the rise of multi- and pan-drug resistant infectious organisms. An important target in this area is the bacterial attachment and subsequent biofilm formation on medical devices (e.g., catheters). Here we describe nonfouling, lubricant-infused slippery polymers as proof-of-concept medical materials that are based on oil-infused polydimethylsiloxane (iPDMS). Planar and tubular geometry silicone substrates can be infused with nontoxic silicone oil to create a stable, extremely slippery interface that exhibits exceptionally low bacterial adhesion and prevents biofilm formation. Analysis of a flow culture of *Pseudomonas aeruginosa* through untreated PDMS and iPDMS tubing shows at least an order of magnitude reduction of biofilm formation on iPDMS, and almost complete absence of biofilm on iPDMS after a gentle water rinse. The iPDMS materials can be applied as a coating on other polymers or prepared by simply immersing silicone tubing in silicone oil, and are compatible with traditional sterilization methods. As a demonstration, we show the preparation of silicone-coated polyurethane catheters and significant reduction of *Escherichia coli* and *Staphylococcus epidermidis* biofilm formation on the catheter surface. This work represents an important first step toward a simple and effective means of preventing bacterial adhesion on a wide range of materials used for medical devices.

**KEYWORDS:** nonfouling material, biofilm prevention, slippery surfaces, nosocomial infection, medical materials



## INTRODUCTION

Through billions of years of evolution, bacteria have developed an arsenal of survival mechanisms against physical and chemical attack.<sup>1,2</sup> One key mechanism facilitating survival is the phenomenon of biofilm formation, whereby planktonic organisms adhere to surfaces and form strongly attached, shear-resistant, matrix-embedded multicellular communities.<sup>3</sup> Biofilms can form on almost any surface in a wide variety of nutrient and flow conditions and, once established, show remarkable resistance to removal.<sup>4,5</sup>

Microbial biofilm formation causes significant problems, particularly in clinical settings. The NIH estimates that biofilms account for over 80% of microbial infections in the body.<sup>6</sup> A pathogenic biofilm resists destruction by both the native immune system and antibiotics<sup>7,8</sup> and leads to serious host infections.<sup>1,9–11</sup> In addition, bacterial pathogens are becoming increasingly insensitive to our therapies, making the added drug resistance of pathogenic biofilms even more dangerous. In particular, Gram-negative *Pseudomonas aeruginosa* causes 10–15% of nosocomial (hospital-acquired) infections worldwide,<sup>12,13</sup> has high intrinsic drug resistance and exhibits virtually all known mechanisms of adaptive resistance to new therapies.<sup>14</sup> Other clinically relevant pathogens that pose similar challenges include *Escherichia coli*<sup>15</sup> and *Staphylococcus*

*epidermidis*,<sup>16</sup> and these organisms are also investigated herein. Hence, a “physical”, noncytotoxic approach to preventing bacterial adhesion is of great significance, because it can avoid the problems of selection pressures for drug resistance of these organisms.<sup>17–19</sup> Biofilm formation has a causal link with nearly all nosocomial infections, and reducing the bacterial colonization on the surface of medical materials in a simple and sustainable way is of immense importance to healthcare systems across the world. For example, urinary tract infection (UTI) represents 40% of all nosocomial infections,<sup>20,21</sup> 11% of which are caused by *P. aeruginosa*,<sup>22</sup> and inhibiting biofilm growth on catheter materials could substantially improve this situation.

Previous materials research<sup>23</sup> addressing the bacterial fouling problem has focused on antimicrobial coatings and chemical and structural modifications of solid materials. Antibiotic<sup>24–26</sup> and metal-ion based<sup>27,28</sup> approaches have shown some success in reducing biofilm growth and subsequent infection, however these approaches destroy the bacterial populations and accelerate the emergence of pan-drug resistant pathogens.<sup>29</sup> The roles of hydrophobicity and hydrophilicity in bacterial

**Received:** October 13, 2014

**Accepted:** December 4, 2014

**Published:** December 4, 2014

adhesion have been extensively studied.<sup>30–33</sup> Hydrophobic surfaces generally cause greater initial attachment but easier detachment of settling organisms than hydrophilic surfaces.<sup>30,34,35</sup> Surface topography is also important for both promoting<sup>36</sup> and preventing<sup>37–40</sup> the adhesion of biological species, and subnanometrically smooth titanium surfaces have been shown to reduce bacterial attachment.<sup>41,42</sup> These approaches, however, have had only limited success and have failed to yield highly effective, long-term antibiofouling materials. Antibacterial coatings of medical tubing in particular present an extreme challenge, as both inner and outer surfaces often require structuring or functionalization and access to these surfaces is hindered and problematic.

The lining in the microstructured gastrointestinal tract is coated with a thick liquid mucus layer, which shields and protects the underlying tissue from the colonization by bacterial populations.<sup>2</sup> This provides inspiration for a new class of antibiofouling materials with a surface liquid layer, which is immobilized on a rough solid because of capillary forces and chemical affinity and which creates a low-adhesion interface. Such bioinspired slippery liquid-infused porous surfaces (SLIPS)<sup>43</sup> have shown promising antibacterial performance in a polytetrafluoroethylene (PTFE)-based system,<sup>44</sup> and more recently in fluorogels<sup>45</sup> and vascularized polymer networks.<sup>46</sup> It would be beneficial to design slippery surfaces with a stable and continuously replenishable lubricant layer, particularly for medical tubing and catheter-relevant materials such as polyurethane and silicone and other flow-exposed medical materials, on which bacteria are known to attach and form biofilms within hours.<sup>47</sup> We hypothesized that infusing silicone such as polydimethylsiloxane (PDMS) with a nontoxic and compatible solvent could become a highly practical approach to create a lubricated liquid overlayer that resists bacterial attachment on silicone-based or silicone-coated medical materials.

Unlike the recently reported infused polymers that rely on custom polymers,<sup>48</sup> PDMS is a widely used nontoxic material in the medical sector. It is biocompatible, flexible, and can be rendered slippery when perfused with a large quantity of a lubricating liquid.<sup>49,50</sup> Perfusion/swelling with lubricant provides a reservoir of diffusing oil and helps to ensure longevity of the lubricant layer in the presence of continuous shear forces. We anticipated that initial biofilm formation would be inhibited by an extremely smooth, slippery and mobile liquid surface formed on the silicone. Further, we expected that even if biofilm were to initially form on the lubricant-infused PDMS (iPDMS) surface, it would be easily washed away in a high-shear flow due to a reduced adhesion of the biofilm to the liquid interface. Herein we present iPDMS or iPDMS-coated tubing as an effective, antibiotic-free, nonbiofouling material that can be further developed for applications in indwelling catheters and other medical devices.

## 1. MATERIALS AND METHODS

**1.1. Flat Silicone Sample Preparation.** Flat silicone samples (Dow Sylgard 184 polydimethylsiloxane, PDMS) were produced for contact and sliding angle characterization. Prepolymer was mixed with curing agent in a 10:1 ratio, mixed in a dual centrifuge mixer, poured into the bottom of a flat Petri dish, and degassed for 1 h in a vacuum chamber. The sample was cured for 4 h at 70 °C before being peeled away from the Petri dish. The control samples were used without further treatment. The infused silicone (iPDMS) samples were prepared by immersing the cured PDMS in 5 cSt silicone oil (Sigma-Aldrich) overnight before analysis.

**1.2. Silicone Tubing Sample Preparation.** Masterflex brand peroxide-cured silicone tubing having inner diameter of 6.4 mm (Cole Parmer, Masterflex L/S 17) was submerged in 5 cSt silicone oil overnight (~16 h) to prepare iPDMS tubing samples used in antibiofouling characterization. Prior to swelling, three 1 m sections of silicone tubing were sterilized by autoclaving for 15 min at 121 °C. Silicone oil was sterile filtered through a Millipore 0.2  $\mu$ m filter unit. The tubing samples were aseptically transferred into the sterile silicone oil bath and left overnight. Control tubing samples were sterilized using the same autoclaving cycle before use.

**1.3. Silicone-Coated Polyurethane Catheter Sample Preparation.** Dual lumen polyurethane catheters (OD 0.16 mm) were first rinsed with ethanol and dried. In order to firmly attach silicone and to prevent delamination of iPDMS, a prime coat (Dow Corning, Sylgard 1205 Prime Coat) was applied by wiping with a tissue moistened with it and cured at room temperature for 2 h. The prime coat is mostly based on allyltrimethoxysilane, which forms cross-linked network of polysiloxane layer. After curing the prime coat, PDMS (Dow Sylgard 184) prepolymer was applied by spray or dip coating and cured at 70 °C for 2 h. The viscosity of the PDMS prepolymer mixture was adjusted using a hexamethyldisiloxane-based silicone solvent (Smooth-On, NOVOCS Gloss Silicone Solvent). The silicone-coated polyurethane catheter was then immersed in 5 cSt silicone oil overnight to prepare iPDMS-coated polyurethane catheter samples (see Figure S1 in the Supporting Information). To visualize the iPDMS coating layer, Oil Red O (Sigma-Aldrich) dye was premixed with the PDMS prepolymer or the silicone solvent. All treated catheter samples were sterilized using the same autoclave cycle used for silicone tubing samples.

**1.4. Contact Angle Characterization.** Contact angles were measured on flat silicone substrates using a goniometer (KSV Instruments, CAM 101). iPDMS samples were hung vertically and then placed on absorbent paper to remove excess lubricant before characterization. For each static contact angle measurement, a 15  $\mu$ L deionized water droplet was placed on the substrate surface and the static contact angle was obtained using Young–Laplace curve fitting; this was repeated 10 times on different areas of one PDMS sample. A precision syringe with a 20G blunt needle was used to expand and contract a water droplet, which was imaged and analyzed to obtain the advancing and receding contact angles, respectively. Advancing and receding contact angles were measured 10 times, averaged, and subtracted from each other to obtain a contact angle hysteresis value.

**1.5. Sliding Angle Characterization.** A sliding stage with a digital protractor was used to measure the sliding angle of a 20  $\mu$ L droplet of water on the surface of each flat silicone substrate. To remove any dust and other contaminants, we gently washed the samples with deionized water and then air-dried them. For each measurement, the angle was slowly increased until the droplet began to slide along the surface, at which point the sliding angle was noted; this was repeated 10 times on different areas of the PDMS sample.

**1.6. Adhesion Force Measurements.** The coefficient of friction for iPDMS was measured according to the ASTM standard D1894–14. A digital force gauge (Mark-10, Series 4) was mounted on a syringe pump (Harvard Apparatus, PHD ULTRA) to pull a polished 2.5''  $\times$  2.5'' aluminum sled (McMaster-Carr, alloy 6061) of 0.1 kg for a distance of 2.5'' across a 6 7/8''  $\times$  6 7/8'' iPDMS sample at a constant rate of 150 mm/min. A nylon monofilament (Trilene, 3.6 kg max. load capacity and 0.012'' avg. diameter) was used as a towline. PDMS samples were immersed in silicone oil for >16 h and spun with a spin coater (Specialty Coating Systems, Spin-coat G3P-15) at 1000 rpm for 60 s to ensure consistent lubricant overlayer thickness in all tested iPDMS samples.

**1.7. Lubricant Removal through Evaporation.** Accelerated and uniform removal of the lubricant was accomplished by placing fully infused iPDMS samples in an oven at 70 °C. Samples were gently wiped prior to the experiment to remove any excess lubricant from the surface. The masses of the samples were then taken daily using a Mettler Toledo Xs205 DualRange analytical balance to measure lubricant loss via evaporation.

**1.8. Lubricant Replenishment Characterization.** The surface of the sample was imaged using phase-contrast optical microscopy at low magnification to observe the coverage of the surface liquid layer. The surface was wiped dry using an absorbent wipe and imaged every hour for a 24 h period. The images provided are typical examples of the flat iPDMS samples.

**1.9. Flow-Based Biofilm Experiment.** GFP-expressing *P. aeruginosa* PA14 were cultured in Difco Miller LB Broth (Becton, Dickinson and Company) overnight, shaking at 37 °C. The cultures were then diluted 1:100 into 350 mL of LB Broth +0.2% (w/v) sodium citrate in a 500 mL Erlenmeyer flask and stirred. The sterile silicone tubing was installed in triplicate: for each tube, the inlet was submerged in the inoculated media, the middle section was mounted in a peristaltic pump head, and the outlet was located above the media to ensure biofilms formed only on the inside of tubes at known shear rates. The peristaltic pump (Cole Parmer) has the capability of pumping three tubes simultaneously at a rate of 0.1–100.0 rpm, which respectively produce the “low” (5.5 mL/min) and “high” (150 mL/min) shear rates for the larger swollen tubing (Table 1). After inoculating the stirred media, the experiment began when the media started flowing from the end of the silicone tubing.

**Table 1. Studied Shear Rates for Biofilm Growth**

shear condition	shear rate (s <sup>-1</sup> )	flow rate (mL/min) iPDMS tubing	flow rate (mL/min) untreated tubing
low	10.0	1.75	5.55
medium	47.8	8.39	26.50
high	270.4	47.50	150.03

**1.10. Static Biofilm Experiments.** *S. epidermidis* (ATCC 12228) and *E. coli* (ATCC 25922) were placed at a density of  $\sim 10^7$  cells/mL in tryptic soy broth medium containing 1.5% NaCl. Polyurethane catheters capped at both ends and coated with iPDMS were then added to the dishes and allowed to incubate at 37 °C for 48 h. Upon removal, the catheter pieces were directly stained with crystal violet (CV) in the same manner as the samples from the flow experiments described below.

**1.11. Crystal Violet Staining.** At each time point, the flow was briefly stopped and a 3.8 cm section of tubing was cut from each tube. The sections were vertically dipped into a scintillation vial containing tap water three times. The tubes were then vertically submerged in 0.1% CV solution and incubated for 15 min. Next, the nonspecific stain was washed from the tubes by consecutively dipping the short tubing sample three times into each of three scintillation vials filled with fresh tap water. Finally, a flow of dry nitrogen gas was gently applied to the inner tube surface to dry the stained biofilm.

For analysis of the stained and dried biofilms, the tubes were held vertically in binder clips, photographed, and filled with 95% ethanol.<sup>51</sup> After a 15 min incubation the ethanol was gently mixed using a pipet and diluted 2× into a final volume of 200  $\mu$ L in one well of a flat-bottom 96 well plate. A plate reader was used to measure absorbance of each well at 580 nm, and further 2× dilutions were made for any values above 3. Values were normalized to inner circumference of the tubing to account for differences in surface area between infused and untreated tubing.

**1.12. Confocal microscopy characterization.** Biofilms formed after 48 h in the low shear condition were dried with gently flowing dry nitrogen to remove the media and free-floating organisms (experiment was done in parallel with the crystal violet assay) and directly imaged with an upright confocal microscope (Zeiss, LSM 700) using a water immersion lens. Reported images are representative of the three tubes used for each experiment.

**1.13. Statistics.** Throughout the text, significance is stated for comparisons with  $p < 0.01$  according to a two-tailed Student's *t* test. Reported values in figures and the text are mean values, and error bars or  $\pm$  values are standard deviation (SD). Important statistical comparisons can be found in [Tables S1 and S2](#). For material characterization, comparisons were made between the untreated and

iPDMS samples for the static contact angle, contact angle hysteresis, and sliding angle experiments. Comparisons were also made between untreated and iPDMS samples in the biofouling experiments at all shear rates and in the washing experiment.

## 2. RESULTS AND DISCUSSIONS

In this study we infused commercially available silicone tubing with high-purity silicone oil (kinematic viscosity 5 cSt). The infused silicone oil that permeates the polymer matrix forms a smooth lubricant layer over the surface (Figure 1A–C). This tubing was used to investigate the attachment of *P. aeruginosa* in peristaltic flow (Figure 1D, E).

**2.1. Characterization of Flat iPDMS.** To accurately characterize the hydrophobicity and smoothness of the iPDMS, we measured water static contact angle, contact angle hysteresis, and sliding angle for infused and untreated flat silicone substrates (Figure 2). The water static contact angle for the polymer increased by only 3% after oil infusion (see [Table S1](#) for statistical comparisons of characterization data). However, contact angle hysteresis (CAH, the difference between the advancing and receding angle of a sliding water droplet) of the iPDMS samples was significantly lower than that of untreated controls. CAH is a direct indicator of nonsticky property (or “slipperiness”<sup>52</sup>) of a solid surface. The significant reduction of CAH indicates that the infused silicone oil forms a smooth, defect-free lubricating layer over the solid substrate, effectively eliminating pinning points of the dry surface and reducing the adhesion of liquid droplets.

To quantify the increased slipperiness, we measured the sliding angle of a 20  $\mu$ L water droplet and the coefficient of friction on infused and untreated flat silicone substrates (Figure 2). The untreated sample exhibits a high sliding angle ( $40.1 \pm 9.0^\circ$ ) and much higher measurement variance, both of which suggest a heterogeneous surface with many defects and pinning points. In contrast, the iPDMS exhibits extremely low sliding angle ( $2.1 \pm 0.9^\circ$ ) typical of a smooth, defect-free surface. Furthermore, we measured the coefficient of static and dynamic friction of the iPDMS to be  $0.46 \pm 0.07$  and  $0.40 \pm 0.07$ , respectively, which is much lower than that of standard PDMS (0.98).<sup>53</sup> Measurements after water jet cleaning (30 s) and nitrogen blow drying the iPDMS surface to remove most of the lubricant overlayer as well as particles on the surface showed coefficients of static and dynamic friction to be  $0.37 \pm 0.05$  and  $0.37 \pm 0.06$ , respectively. This indicates that even after forced removal of the apparently visible lubricant overlayer, there still exists a thin and smooth lubricant layer on the top of the iPDMS surface. This lubricant layer is seen in the confocal microscopy images of the PDMS infused with Oil Red O dye-loaded oil.

Maintaining the slippery properties of the iPDMS requires the continued presence of the surface liquid layer. Since this layer can be removed by shear force, it is beneficial to have a large “reservoir” of solvent within the material from which the surface lubricant layer can be replenished. We have recently demonstrated this diffusion-based self-lubricating phenomenon to occur in a lubricant-infused fluorogel system.<sup>50</sup> The diffusion of oil to the interface upon the removal of the surface lubricant layer was further confirmed by the microscopy experiments (Figure 3A): the iPDMS surface was swabbed dry with an absorbent wipe and the steady reappearance of the silicone oil on the surface was observed. This proves the concept of keeping the slippery performance via self-replenishment from



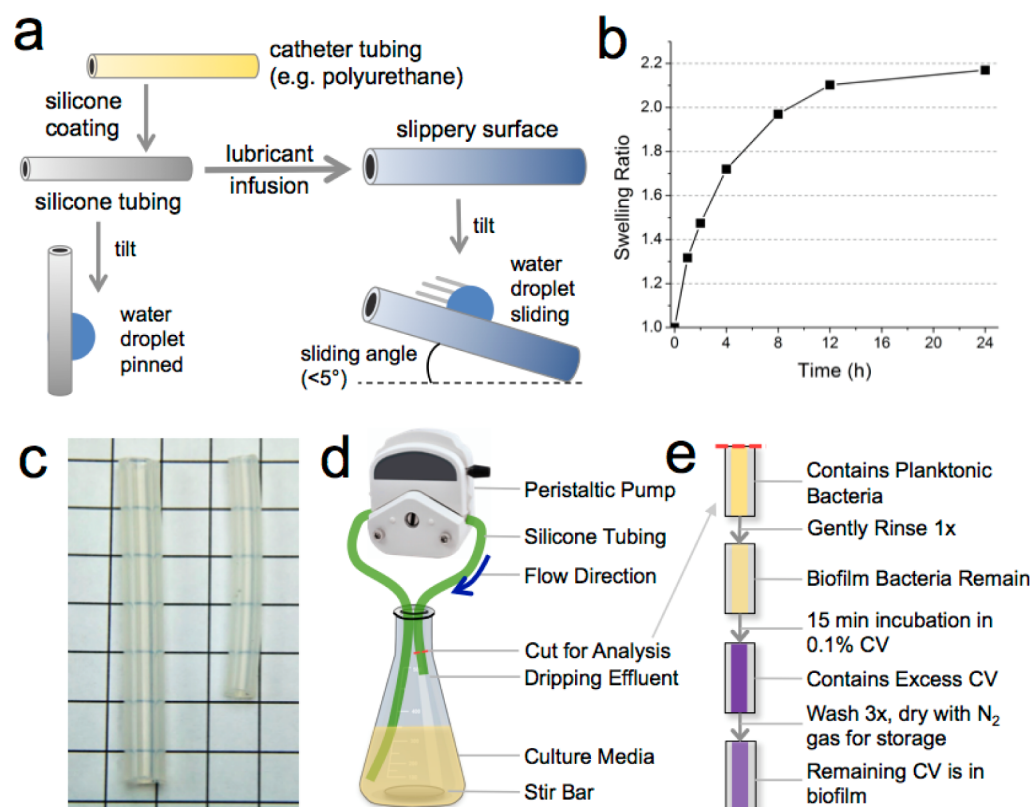


**Figure 1.** Analysis of dry and oil-infused PDMS tubing as an antibiofouling surface. (a) Silicone tubing, either as an overcoat applied on other materials (e.g., polyurethane) or as a tubing made of silicone itself, can be infused with lubricant (e.g., silicone oil) by immersion. The swollen and infused material (iPDMS) is an extremely slippery material on which droplets can easily slide, whereas they are strongly pinned on the polymer before lubricant infusion. (b) Commercial silicone sample used in this study approaches a maximal swelling ratio of  $2.17 \pm 0.01$  in 24 h ( $n = 3$ , mean  $\pm$  SD, error bars too small to display on figure). (c) Photographs show the larger iPDMS tube (left) beside a smaller untreated tube (right). Before infusion and swelling, both tubes were equal size; swelling increases the unconstrained dimensions of a silicone sample by a factor of 1.4. (d) Schematic showing experimental setup for the investigation of biofilm formation in flow. (e) Schematic illustrating the customized steps used in the crystal violet (CV) staining procedure. The stained biofilm was subsequently solubilized and analyzed with standard methods as described.

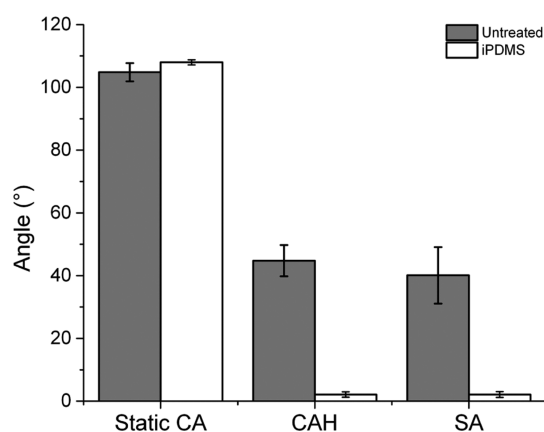


**Figure 2.** Contact angle (CA) characterization of dry and iPDMS substrates. Water static contact angle (CA), CA hysteresis (CAH), and sliding angle (SA) for infused and untreated flat silicone substrates ( $n = 10$ , values are mean  $\pm$  SD). Please refer to Table S2 for raw data and statistical tests. The surface of the iPDMS exhibits significantly lower water contact angle hysteresis and sliding angle with a smaller standard deviation than the untreated silicone surface.

within the polymer where a large amount of lubricant can be stored.

**2.2. Characterization of iPDMS Tubing.** When immersed in a compatible solvent such as silicone oil, PDMS becomes

expanded and infused because the polymer chains extend to maximize polymer–solvent interactions. Further, silicone is particularly amenable to solvent infusion due to the low rotational energy barrier around the  $\text{Me}_2\text{Si}-\text{O}$  bond (3.3 kJ/mol compared to 13.8 kJ/mol around  $-\text{CH}_2-$  in polyethylene) that allows very easy diffusion throughout the polymer matrix. We defined these physical changes by the mass swelling ratio, SR, attributable to the uptake of the solvent

$$\text{SR} = \frac{M_i}{M_u} \quad (1)$$

where  $M_i$  is the mass of the infused polymer (mass of oil + mass of polymer) and  $M_u$  is the mass of the untreated polymer before swelling. The silicone tubing and silicone oil pairing used in this study resulted in an infused polymer with increased mass and volume, reaching an equilibrium, plateaued SR of  $\sim 2.17$  after immersion for 24 h (Figure 1B). The inner diameter of the iPDMS tubing was  $\sim 50\%$  larger than that of the untreated tubing and the length increased by  $\sim 30\%$  after oil infusion (Figure 1C). Importantly, the lubricant-infused state was relatively stable when exposed to continuous flow, with a SR maintained above 1.80 even after a 96-h exposure to a “medium” shear rate ( $47.8 \text{ s}^{-1}$ ) flow (Figure 3B). The surface at this SR remained noticeably slippery because of the self-replenishment mechanism depicted in Figure 3A.

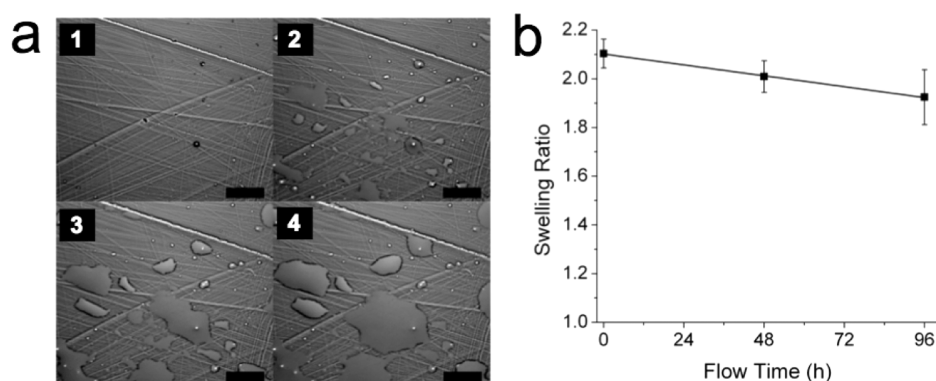


**Figure 3.** Self-replenishment of lubricant overlayer and the longevity of iPDMS tubing under flow. a. Optical images of the restoration of the liquid overlayer of iPDMS. Phase contrast images were obtained of a typical iPDMS surface 0, 1, 6, and 24 h (1–4, respectively) after removal of the surface silicone oil with an adsorbent tissue. Scale bars are 100  $\mu\text{m}$ . b. Deswelling experiment by forced removal of lubricant by shear forces from flowing liquid. iPDMS tubes were exposed to flowing tap water at the medium shear rate ( $\gamma = 47.8 \text{ s}^{-1}$ ). The samples linearly deswell ( $y = 2.100 - 0.002x$ ,  $R^2 = 0.997$ ) over 4 days. After 48 h, the tubes deswell to a swelling ratio of  $1.8 \pm 0.1$  (mean  $\pm$  SD), but the surface remained slippery.

For iPDMS to be a relevant, long-term slippery material for biomedical applications such as catheters, it must show continuous resistance to bacterial adhesion and suitable physical properties. Forced removal of lubricant by evaporation from a fully swollen iPDMS showed that a reduction of the mass of infused oil of 5–10% removes the nonfouling properties of iPDMS in a *static* culture (Figure S2) when tested immediately ( $<5$  min) without allowing self-replenishment to take place; similar level of lubricant loss can occur after 48 h of continuous exposure to the medium shear rate. The minimal biofilm adhesion in the high shear rate (under which lubricant loss can be even greater than 10% in 48 h) indicates that higher shear forces enable nonbiofouling performance despite greater lubricant loss. In physiologically relevant flow conditions present in long-term catheterization scenarios, urine slowly leaves the bladder and creates a low shear condition at the tubing wall, thus causing substantially lower degradation of nonfouling function due to the loss of the lubricant. It is noteworthy that oil-containing PDMS coatings exposed to natural ambient flow in marine environments retained their antifouling capability<sup>54</sup> and effectively prevented marine microfouling within at least a year.<sup>55</sup> Because biofouling of traditional catheters unavoidably occurs when used for extended periods of time (e.g.,  $>4$  days), iPDMS could provide an unmatched nonfouling function for an extended period of time in silicone or silicone-coated medical devices.

### 2.3. Antibiofouling Performance of iPDMS Tubing.

**2.3.1. Crystal Violet Assay.** To mimic clinically relevant shear conditions for biofilm formation in and on catheters, we flowed *P. aeruginosa*-containing culture (strain PA14) through iPDMS and untreated PDMS tubing and analyzed bacterial attachment at three different shear rates, ranging from 10.0 to 270.4  $\text{s}^{-1}$  simply referred to here as “low”, “medium”, and “high” (Table 1). It was necessary to monitor shear rate instead of using flow rate because the inner diameters of the tubes were different. For a larger internal diameter, higher flow rates are required to achieve the same shear forces at the internal wall, as shown in eq 2<sup>56</sup>

$$\gamma = \frac{4Q}{\pi r^3} \quad (2)$$

where  $\gamma$  is the shear rate ( $\text{s}^{-1}$ ),  $Q$  is the volumetric flow rate, and  $r$  is the inner radius of the tube.

We pumped a stirred culture of *P. aeruginosa* through the tubing continuously. At 0, 8, 24, and 48 h time points, we cut off a 1.5 in. section from the end of the tubings and quantified the amount of biofilm present with crystal violet (CV) staining (Figure 1D, E). In all three shear conditions, at all time points, the iPDMS tubing exhibited substantially reduced biofilm growth relative to the untreated control tubing (Figure 4A, B), based on a quantitative CV assay (see Table S2 for raw data and statistical comparisons for the 48 h time point). Note that some biofilm aggregates did form in the low shear condition, however their morphology was very different (Figure 4B) from the thick, uniform coating seen on the untreated tubing and the biofilm was easily removed with a simple washing step (Figure 4C). Both of these indicate that the bacterial aggregates form on top of a stable silicone oil layer. To further investigate how strongly these biofilms adhere to untreated and iPDMS tubing, we examined the effect of a simple washing step (a 10 s exposure to flowing tap water) on attached biofilms (Figure 4C) grown in the low shear condition. Analysis by CV assay confirmed that the biofilm was removed from the surface of the iPDMS tubing in less than 5 s, whereas the same wash had a comparatively small effect on the control tubing (see Table S2, Figure 4C). Extending the wash to 5 min, there was still only a small reduction in biofilm coverage on the surface of the control tubing, indicating strong adherence and the presence of a more mature, robustly attached biofilm.

**2.3.2. Confocal Microscopy Study of the Biofilm Morphology.** To further probe how bacteria interact and reside at the lubricant overlayer interface, we grew green fluorescent protein (GFP)-expressing *P. aeruginosa* to form biofilms for 48 h in the low shear condition on the substrates. After the growth, iPDMS and control tubing samples were air-dried and imaged with an upright confocal microscope (note that no visible biofilm is formed at medium and high shear conditions on iPDMS). The biofilm on the untreated PDMS tubing appears to be relatively flat, homogeneous, on the order of 10–100  $\mu\text{m}$  thick, and inhabited by a dense cellular community (Figure 5A–D). Observing the cross-section of the film does not reveal any bacteria below the outer surface of the tubing. On the other hand, the bacteria attached to the iPDMS tubing are limited to small loosely attached bacterial aggregates and isolated cells within the lubricant layer of the tubing itself. These bacteria appear to be planktonic as indicated by their low density and mutual isolation, which shows that the bacteria are unable to

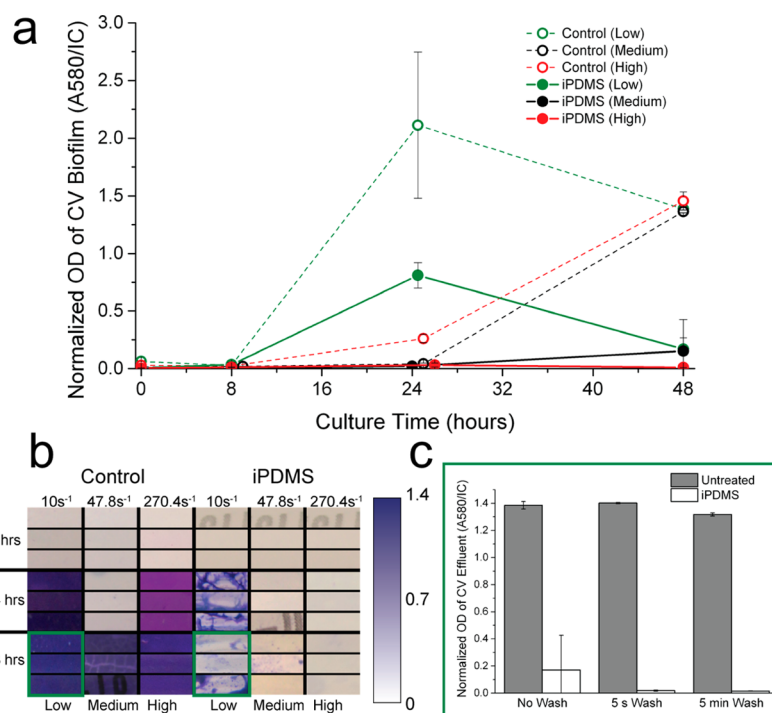


**Figure 4.** Attachment of *P. aeruginosa* biofilms to infused and untreated silicone tubing. (a) Normalized absorbance values of CV-stained biofilms grown under low, medium and high shear rates for 0, 8, 24, and 48 h. Biofilm volume was determined by measuring the absorbance ( $\lambda = 580$  nm) of retained crystal violet (CV) in each sample. (Mean  $\pm$  SD, raw data and statistical tests are available in Table S2). (b) Photographs of CV-stained tubes; purple color reflects the presence of biofilms. Note the reduced amount of biofilms on iPDMS tubing samples, particularly at the high shear rate. (c) Presence of biofilms after a washing step. Biofilms were grown in the low shear condition for 48 h and “washed” in the high shear condition for 5 s and 5 min and analyzed using the CV assay. Note that urinary catheters, for example, allow free drainage of the bladder as urine is produced, which is a slow process that is modeled here with the low shear condition.

sense and adhere to a solid surface.<sup>57</sup> It was difficult to discern the precise location of the bacteria, whether above, within, or below the lubricant overlayer due to the extremely small thickness of the lubricant layer<sup>43</sup> and the challenge associated with selective fluorescent labeling of the lubricant layer alone. Note that it has been previously shown that the thickness of a surface-stabilized liquid layer on a rough surface increases from 10 nm to 1  $\mu$ m as roughness increases,<sup>58</sup> indicating that this property is tunable if necessary. Although this characterization clearly demonstrates the morphological differences between the two samples and the reduction of biofilm, further investigations such as genetic analysis, slime staining, or other imaging methods to confidently discern the state and the depth of the embedded bacteria as well as the precise thickness of lubricant overlayer would provide a clear picture for understanding the detailed mechanism of bacterial interaction and nonfouling effect of iPDMS systems.

Experiments performed with polyurethane catheters coated with the iPDMS surface layer and tested under static conditions with *S. epidermidis* and *E. coli* showed antifouling results similar to those observed with iPDMS tubing (Figure S3).

**2.4. On the Mechanism of the Antibacterial Function of iPDMS and iPDMS-Coated Materials.** The ease with which biofilm is removed from the iPDMS surface suggests a removal mechanism that is very different from that observed with solid surfaces, due to a combination of smoothness, slipperiness, and the presence of the liquid layer. It has been shown that the presence of a liquid overlayer decreases the apparent roughness of the material dramatically,<sup>43</sup> and this effect likely reduces the mechanical triggers for bacterial biofilm formation. With regards to slipperiness, it is important to note

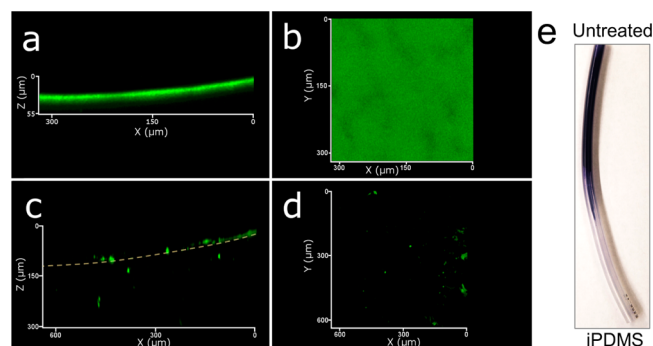


**Figure 5.** Confocal Images of typical *P. aeruginosa* biofilms on untreated and infused silicone tubing. (A, B) Bacteria readily form a  $\sim 40$   $\mu$ m thick biofilm on untreated silicone tubing. (C, D) Biofilms are not present on the surface of iPDMS tubing in the same conditions. Note that some small, easily removed bacterial aggregates are present on the surface, and that isolated bacteria entered the walls of the infused tubing. (E) Photograph of CV-stained biofilms formed on variably infused silicone tubing in the same conditions as A–D; the lower half is infused and the top half is untreated. Only a very small amount of biofilms form on the infused section of the tube, and biofilms are clearly present on the untreated section.

that low friction surfaces only affect adhesion by reducing the friction pathogens experience when in contact with the media-lubricating oil interface. This increased speed at the boundary reduces the normal adhesion forces that allow pathogens to adhere to solid surfaces, thus inhibiting attachment behavior.<sup>59</sup> It is possible that the bacteria slide along the inner wall of the tubing with much lower resistance than experienced in



unmodified PDMS.<sup>60</sup> On the other hand, bacteria on the iPDMS surface could become encased in silicone oil (which itself might inhibit biofilm production by blocking signals between organisms<sup>61</sup>) and removed through an emulsion when exposed to sufficiently high shear forces.

This hints at the deeper question regarding the stability of the iPDMS liquid overlayer; some insight here can be provided by recent investigations into core annular flow (the use of lubricating oil on the inner pipe wall) as a means of reducing friction in liquid flow systems.<sup>62–64</sup> Although high fluid shear rates lead to turbulent flow and instability of the liquid–oil interface, this effect was reduced in close proximity to the solid inner wall of the tubing.<sup>62,64</sup> Such liquid instability can be seen millimeters away from the tubing wall, which indicates that the much thinner layer of lubricating oil in iPDMS could be stable, especially at lower shear rates. Further, our experiments (Figure S2) show that even at zero shear rate (static conditions) biofilm formation is minimal, and those films that do form are easily washed away. This indicates that the outer interface between water and the liquid silicone overlayer is stable in static and low-shear conditions.

## ■ CONCLUSIONS

Silicone is already used in myriad medical applications, including indwelling catheters and cardiac and pulmonary tubing because of its high biocompatibility and desirable clinical performance.<sup>65–67</sup> By simple immersion in silicone oil, an extremely easy and reproducible treatment protocol, the silicone-based materials and coatings gain a slippery, long-lasting lubricated surface (iPDMS) that significantly reduces biofouling. We have demonstrated that *P. aeruginosa* biofilm formation can be reduced in various shear conditions, including those representative of indwelling catheters, by at least 10-fold. After a 5 s wash with water, the biofilm volume can be almost completely removed from iPDMS, while a robust biofilm remained on the untreated control silicone surfaces (Figure SE). Further, the iPDMS materials passively resist bacterial accumulation without the use of bactericidal agents, and could thus be developed as an important component in reducing excessive antibiotic usage.

Our results illustrate that shear forces can substantially decrease the initial formation of *P. aeruginosa* biofilms on the surface of iPDMS while also enabling the subsequent removal of biofilms that are present. Even at low shear conditions close to a static culture, a significant reduction in biofilm was observed. Since the hydrophobicity remains essentially unchanged after lubricant infusion, this could conceivably be explained by the fact that the mobile liquid overlayer prevents bacteria from probing and forming bonds on the solid surface and makes it a nonoptimal attachment site for the bacteria. Another possible factor is the increased softness of the solid surface below the liquid layer, as decreasing the material's stiffness was shown to reduce bacterial attachment.<sup>68</sup> Though the underlying mechanisms causing reduced biofilm formation on iPDMS tubing require more thorough investigation to be fully understood, this approach is effective and can be easily implemented. The ability of the infused oil to travel to the interface and replenish the surface liquid overlayer upon removal in flow provides a significant advantage of iPDMS tubing for long-lasting antimicrobial performance.<sup>49</sup> Moreover, the ability to form the vascularized PDMS coatings<sup>46</sup> allows for broad application of this technique even for longer-term

medical devices where the lubricating fluid can be added and be transported through the polymer to the interface.

Another important consideration is the discussion of the toxicity levels of silicone oil to both pathogens and the patient. The Kirby-Bauer test has shown that silicone oil had low toxicity to a range of common pathogenic bacteria including *P. aeruginosa*.<sup>69</sup> In addition, studies on the impact of silicone oil to marine life has shown low toxicity to marine organisms and low bioaccumulation.<sup>61</sup> More relevant to human patients involving safety investigations of silicone breast implants, it has been shown that injected silicone oil is nontoxic on the cellular and systemic levels.<sup>66</sup> These previous studies strongly suggest that the silicone oil lubricant overlayer does not act as a biocide against the bacteria used in this study and does not pose a threat to the health of a potential patient.

These results provide an early indication of the clinical potential of iPDMS as a medical material in general and catheter and tubing material in particular. The lower bacterial attachment, unmatched long-term antibacterial performance and effective disinfection by a simple washing step are all desirable features of an in-dwelling catheter material. The presence of the lubricant overlayer on the catheter surfaces has the additional potential advantage of improving patient comfort during catheter insertion and removal—another substantial drawback of traditional catheters.<sup>70–72</sup> More broadly, iPDMS surface coatings would be beneficial on any material that requires fast, simple and effective elimination of bacterial contamination. Although our proof-of-concept data suggest that long-term nonfouling performance is achievable, more rigorous characterization with additional strains of bacterial species in various other types of media and in more representative physiological conditions would be required before this surface treatment can be fully validated as a medical material. It will also be important to determine the functional lifetime of iPDMS when exposed to various shear forces to confirm the material's clinical viability. We hope this initial work will motivate further investigation into the antifouling and infection-reducing potential of iPDMS, and that the clinical potential of this material can be realized in the future.

## ■ ASSOCIATED CONTENT

### Supporting Information

The following file is available free of charge on the ACS Publications website at DOI: 10.1021/ab5000578.

Photograph of polyurethane catheters with iPDMS coating, biofilm coverage of iPDMS in static conditions, absorbance of CV-stained biofilms grown on iPDMS-coated catheters under static conditions, and raw data and statistical tests for iPDMS characterization and biofouling experiments (PDF)

## ■ AUTHOR INFORMATION

### Corresponding Author

\*E-mail: jaiz@seas.harvard.edu. Phone: (617) 495-3558.

### Author Contributions

The manuscript was written through contributions of all authors. All authors have given approval to the final version of the manuscript.

### Notes

The authors declare no competing financial interest.

## ■ ACKNOWLEDGMENTS

We thank Mr. Jack Alvarenga for materials and equipment management, as well as Gareth Holmes, Haylea Ledoux, and Carine Nemr for their help with the static biofilm studies. This work was supported in part by the Office of Naval Research under award no. N00014-11-1-0641.

## ■ REFERENCES

- (1) Costerton, W. J.; Stewart, P. S.; Greenberg, E. P. Bacterial biofilms: a common cause of persistent infections. *Science* **1999**, *284* (5418), 1318–1322.
- (2) Costerton, J. W.; Lewandowski, Z.; Cladwell, D. E.; Korber, D. R.; Lappin-Scott, H. M. Microbial biofilms. *Annu. Rev. Microbiol.* **1995**, *49* (1), 711–745.
- (3) O'Toole, G.; Kaplan, H. B.; Kolter, R. Biofilm formation as microbial development. *Annu. Rev. Microbiol.* **2000**, *54* (1), 49–79.
- (4) Chen, X.; Stewart, P. S. Biofilm removal caused by chemical treatments. *Water Res.* **2000**, *34* (17), 4229–4233.
- (5) Melo, L. F.; Vieira, M. J. Physical stability and biological activity of biofilms under turbulent flow and low substrate concentration. *Bioprocess Eng.* **1999**, *20* (4), 363–368.
- (6) Romero, R.; Schaudinn, C.; Kusanovic, J. P.; Gorur, A.; Gotsch, F.; Webster, P.; Nhan-Chang, C.-L.; Erez, O.; Kim, C. J.; Espinoza, J.; Gonçalves, L. F.; Vaisbuch, E.; Mazaki-Tovi, S.; Hassan, S. S.; Costerton, J. W.; et al. Detection of a microbial biofilm in intra-amniotic infection. *Am. J. Obstet. Gynecol.* **2008**, *198* (1), 1–11.
- (7) Davies, D. Understanding biofilm resistance to antibacterial agents. *Nat. Rev. Drug Discovery* **2003**, *2* (2), 114–122.
- (8) Costerton, J. W.; Cheng, K. J.; Ladd, T. I.; Nickel, J. C.; Dasgupta, M.; Marrie, T. J. Bacterial biofilms in nature and disease. *Annu. Rev. Microbiol.* **1987**, *41* (1), 435–464.
- (9) Götz, F. Staphylococcus and biofilms. *Mol. Microbiol.* **2002**, *43* (6), 1367–1378.
- (10) Subbiahdoss, G.; Kuijter, R.; Grijpma, D. W.; van der Mei, H. C.; Busscher, H. J. Microbial biofilm growth vs. tissue integration: “The race for the surface” experimentally studied. *Acta Biomater.* **2009**, *5* (5), 1399–1404.
- (11) Senneville, E.; Joulie, D.; Legout, L.; Valette, M.; Dezèque, H.; Bertrand, E.; Roselée, B.; d'Escrivan, T.; Loiez, C.; Caillaux, M.; Yazdanpanah, Y.; Maynou, C.; Migaud, H. Outcome and predictors of treatment failure in total hip/knee prosthetic joint infections due to Staphylococcus aureus. *Clin. Infect. Dis.* **2011**, *53* (4), 334–340.
- (12) Fernández, L.; Gooderham, W. J.; Bains, M.; McPhee, J. B.; Wiegand, I.; Hancock, R. E. W. Adaptive resistance to the “last hope” antibiotics polymyxin B and colistin in *Pseudomonas aeruginosa* is mediated by the novel two-component regulatory system ParR-ParS. *Antimicrob. Agents Chemother.* **2010**, *54* (8), 3372–3382.
- (13) Blanc, D. S.; Petignat, C.; Janin, B.; Bille, J.; Francioli, P. Frequency and molecular diversity of *Pseudomonas aeruginosa* upon admission and during hospitalization: a prospective epidemiologic study. *Clin. Microbiol. Infect.* **1998**, *4* (5), 242–247.
- (14) Hancock, R. E.; Speert, D. P. Antibiotic resistance in *Pseudomonas aeruginosa*: mechanisms and impact on treatment. *Drug Resistance Updates* **2000**, *3* (4), 247–255.
- (15) Rosenthal, V. D.; Todi, S. K.; Álvarez-Moreno, C.; Pawar, M.; Karlekar, A.; Zeggwagh, A. A.; Mitrev, Z.; Udwadia, F. E.; Navoa-Ng, J. A.; Chakravarthy, M.; et al. Impact of a multidimensional infection control strategy on catheter-associated urinary tract infection rates in the adult intensive care units of 15 developing countries: findings of the International Nosocomial Infection Control Consortium (INICC). *Infection* **2012**, *40* (5), 517–526.
- (16) Seral, C.; Yolanda, S.; Algarate, S.; Duran, E.; Luque, P.; Torres, C.; Castillo, F. J. Nosocomial outbreak of methicillin- and linezolid-resistant Staphylococcus epidermidis associated with catheter-related infections in intensive care unit patients. *Int. J. Med. Microbiol.* **2011**, *301* (4), 354–358.
- (17) Snelling, A. M.; Kerr, K. G. *Pseudomonas aeruginosa*: a formidable and ever-present adversary. *J. Hosp. Infect.* **2009**, *73* (4), 338–344.
- (18) Strateva, T.; Yordanov, D. *Pseudomonas aeruginosa*-a phenomenon of bacterial resistance. *J. Med. Microbiol.* **2009**, *58* (9), 1133–1148.
- (19) Poole, K. *Pseudomonas aeruginosa*: resistance to the max. *Front Microbiol.* **2011**, *2*, 65.
- (20) Nicolle, L. E. Urinary catheter-associated infections. *Infect. Dis. Clin. North Am.* **2012**, *26* (1), 13.
- (21) Saint, S.; Chenoweth, C. E. Biofilms and catheter-associated urinary tract infections. *Infect. Dis. Clin. North Am.* **2003**, *17* (2), 411–432.
- (22) Emori, T. G.; Gaynes, R. P. An overview of nosocomial infections, including the role of the microbiology laboratory. *Clin. Microbiol. Rev.* **1993**, *6* (4), 428–442.
- (23) Banerjee, I.; Pangule, R. C.; Kane, R. S. Antifouling coatings: recent developments in the design of surfaces that prevent fouling by proteins, bacteria, and marine organisms. *Adv. Mater.* **2011**, *23* (6), 690–718.
- (24) Raad, I.; Darouiche, R.; Dupuis, J.; Abi-Said, D.; Gabrielli, A.; Hachem, R.; Wall, M.; Harris, R.; Jones, J.; Buzaid, A.; Robertson, C.; Salwa, S.; Curling, P.; Burke, T.; Ericsson, C. Central venous catheters coated with minocycline and rifampin for the prevention of catheter-related colonization and bloodstream infections: a randomized, double-blind trial. *Ann. Int. Med.* **1997**, *127* (4), 267–274.
- (25) Maki, D. G.; Stolz, S. M.; Wheeler, S.; Mermel, L. A. Prevention of central venous catheter-related bloodstream infection by use of an antiseptic-impregnated catheter: A randomized, controlled trial. *Ann. Int. Med.* **1997**, *127* (4), 257–266.
- (26) Pritchard, E. M.; Valentin, T.; Panillaitis, B.; Omenetto, F.; Kaplan, D. L. Antibiotic-Releasing Silk Biomaterials for Infection Prevention and Treatment. *Adv. Funct. Mater.* **2013**, *23* (7), 854–861.
- (27) Novikov, A.; Lam, M. Y.; Mermel, L. A.; Casey, A. L.; Elliott, T. S.; Nightingale, P. Impact of catheter antimicrobial coating on species-specific risk of catheter colonization: a meta-analysis. *Antimicrob. Resist. Infect. Control* **2012**, *1* (1), 1–9.
- (28) Stevens, K. N.; Crespo-Biel, O.; van den Bosch, E. E. M.; Dias, A. A.; Knetsch, M. L. W.; Aldenhoff, Y. B. J.; van der Veen, F. H.; Maessen, J. G.; Stobberingh, E. E.; Koole, L. H. The relationship between the antimicrobial effect of catheter coatings containing silver nanoparticles and the coagulation of contacting blood. *Biomaterials* **2009**, *30* (22), 3682–3690.
- (29) Silver, S. Bacterial silver resistance: molecular biology and uses and misuses of silver compounds. *FEMS Microbiol. Rev.* **2003**, *27* (2–3), 341–353.
- (30) Fletcher, M.; Loeb, G. I. Influence of Substratum Characteristics on the Attachment of a Marine Pseudomonad to Solid Surfaces. *Appl. Environ. Microbiol.* **1979**, *37* (1), 67–72.
- (31) Jacobs, A.; Lafolie, F.; Herry, J. M.; Debroux, M. Kinetic adhesion of bacterial cells to sand: cell surface properties and adhesion rate. *Colloids Surf. B. Biointerfaces* **2007**, *59* (1), 35–45.
- (32) Statz, A. R.; Barron, A. E.; Messersmith, P. B. Protein, cell and bacterial fouling resistance of polypeptoid-modified surfaces: effect of side-chain chemistry. *Soft Matter* **2008**, *4* (1), 131–139.
- (33) Oliveira, S. M.; Song, W.; Alves, N. M.; Mano, J. F. Chemical modification of bioinspired superhydrophobic polystyrene surfaces to control cell attachment/proliferation. *Soft Matter* **2011**, *7* (19), 8932–8941.
- (34) Donlan, R. M. Biofilms and device-associated infections. *Emerg. Infect. Dis.* **2001**, *7* (2), 277.
- (35) Bendinger, B.; Rijnaarts, H. H. M.; Altendorf, K.; Zehnder, A. J. B. Physicochemical cell surface and adhesive properties of coryneform bacteria related to the presence and chain length of mycolic acids. *Appl. Environ. Microbiol.* **1993**, *59* (11), 3973–3977.
- (36) Pereira, M. J. N.; Sundback, C. A.; Lang, N.; Cho, W. K.; Pomerantseva, I.; Ouyang, B.; Tao, S. L.; McHugh, K.; Mwizerwa, O.; Vemula, P. K.; Mochel, M. C.; Carter, D. J.; Borenstein, J. T.; Langer, R.; Ferreira, L. S.; Karp, J. M.; Masiakos, P. T. Combined Surface



Micropatterning and Reactive Chemistry Maximizes Tissue Adhesion with Minimal Inflammation. *Adv. Healthcare Mater.* **2014**, 3 (4), 565–571.

(37) Characklis, W. G.; McFeters, G. A.; Marshall, K. C., Physiological ecology in biofilm systems. In *Biofilms*; John Wiley & Sons: New York, 1990; pp 341–394.

(38) Carman, M. L.; Estes, T. G.; Feinberg, A. W.; Schumacher, J. F.; Wilkerson, W.; Wilson, L. H.; Callow, M. E.; Callow, J. A.; Brennan, A. B. Engineered antifouling microtopographies - correlating wettability with cell attachment. *Biofouling* **2006**, 22 (1), 11–21.

(39) Epstein, A. K.; Wong, T.-S.; Belisle, R. A.; Boggs, E. M.; Aizenberg, J. Liquid-infused structured surfaces with exceptional anti-biofouling performance. *Proc. Natl. Acad. Sci. U.S.A.* **2012**, 109 (33), 13182–13187.

(40) Friedlander, R. S.; Vlamakis, H.; Kim, P.; Khan, M.; Kolter, R.; Aizenberg, J. Bacterial flagella explore microscale hummocks and hollows to increase adhesion. *Proc. Natl. Acad. Sci. U. S. A.* **2013**, 110 (14), 5624–5629.

(41) Ivanova, E. P.; Truong, V. K.; Wang, J. Y.; Berndt, C. C.; Jones, R. T.; Yusuf, I. I.; Peake, I.; Schmidt, H. W.; Fluke, C.; Barnes, D.; Crawford, R. J. Impact of nanoscale roughness of titanium thin film surfaces on bacterial retention. *Langmuir* **2009**, 26 (3), 1973–1982.

(42) Puckett, S. D.; Taylor, E.; Raimondo, T.; Webster, T. J. The relationship between the nanostructure of titanium surfaces and bacterial attachment. *Biomaterials* **2010**, 31 (4), 706–713.

(43) Wong, T. S.; Kang, S. H.; Tang, S. K. Y.; Smythe, E. J.; Hatton, B. D.; Grinthal, A.; Aizenberg, J. Bioinspired self-repairing slippery surfaces with pressure-stable omniphobicity. *Nature* **2011**, 477 (7365), 443–477.

(44) Epstein, A. K.; Wong, T.-S.; Belisle, R. A.; Boggs, E. M.; Joanna, A. Liquid-infused structured surfaces with exceptional anti-biofouling performance. *Proc. Natl. Acad. Sci. U.S.A.* **2012**, 109 (33), 13182–13187.

(45) Yao, X.; Dunn, S. S.; Kim, P.; Duffy, M.; Alvarenga, J.; Aizenberg, J. Fluorogel Elastomers with Tunable Transparency, Elasticity, Shape and Memory, and Anti-fouling Properties. *Angew. Chem.* **2014**, 53, 1–6.

(46) Howell, C.; Vu, T. L.; Lin, J. J.; Kolle, S.; Juthani, N.; Watson, E.; Weaver, J. C.; Alvarenga, J.; Aizenberg, J. Self-Replenishing Vascularized Fouling-Release Surfaces. *ACS Appl. Mater. Interfaces* **2014**, 6 (15), 13299–13307.

(47) Stickler, D. J.; Morris, N. S.; McLean, R. J. C.; Fuqua, C. Biofilms on Indwelling Urethral Catheters Produce Quorum-Sensing Signal Molecules In Situ and In Vitro. *Appl. Environ. Microbiol.* **1998**, 64 (9), 3486–3490.

(48) Li, J.; Kleintschek, T.; Rieder, A.; Cheng, Y.; Baumbach, T.; Obst, U.; Schwartz, T.; Levkin, P. A. Hydrophobic Liquid-Infused Porous Polymer Surfaces for Antibacterial Applications. *ACS Appl. Mater. Interfaces* **2013**, 5 (14), 6704–6711.

(49) Eifert, A.; Paulsen, D.; Varanakkottu, S. N.; Baier, T.; Steffen, H. Simple Fabrication of Robust Water-Repellent Surfaces with Low Contact-Angle Hysteresis Based on Impregnation. *Adv. Mater. Interfaces* **2014**, 1–5 DOI: 10.1002/admi.201300138.

(50) Yao, X.; Ju, J.; Yang, S.; Wang, J.; Jiang, L. Temperature-Driven Switching of Water Adhesion on Organogel Surface. *Adv. Mater.* **2014**, 26, 1895–1900.

(51) O'Toole, G. A.; Pratt, L. A.; Paula, W. I.; Newman, D.; Weaver, V. B.; Roberto, K. Genetic approaches to study of biofilms. In *Methods in Enzymology*; Elsevier: Amsterdam, 1999; Vol. 310, pp 91–109.

(52) Li, F.; Mugele, F. How to make sticky surfaces slippery: Contact angle hysteresis in electrowetting with alternating voltage. *Appl. Phys. Lett.* **2008**, 92 (24), 244108.

(53) Chawla, K.; S. L.; BP, L.; JL, D.; PB, M.; ND, S. A novel low-friction surface for biomedical applications: Modification of poly (dimethylsiloxane)(PDMS) with polyethylene glycol (PEG)-DOPA-lysine. *J. Biomed. Mater. Res., Part A* **2009**, 90 (3), 742–749.

(54) Kavanagh, C.; Swain, G.; Kovach, B.; Stein, J.; Darkangelo-Wod, C.; Truby, K.; Holm, E.; Montemarano, J.; Meyer, A.; Wiebe, D. The

Effects of Silicone Fluid Additives and Silicone Elastomer Matrices on Barnacle Adhesion Strength. *Biofouling* **2003**, 19, 381–390.

(55) Truby, K.; Christina, W.; Stein, J.; Cella, J.; Carpenter, J.; CKavanagh, C.; Swain, G.; et al. Evaluation of the performance enhancement of silicone biofouling-release coatings by oil incorporation. *Biofouling* **2000**, 15 (1–3), 141–150.

(56) Darby, R. *Chemical Engineering Fluid Mechanics*; CRC Press: Boca Raton, FL, 2001.

(57) Busscher, H.; van der Mei, H., How do bacteria know they are on a surface and regulate their response to an adhering state? *PLoS Pathog.* **2012**, 8 (1).10.1371/journal.ppat.1002440

(58) Gutt, C.; Sprung, M.; Fendt, R.; Madsen, A.; Sinha, S.; Tolan, M., Partially Wetting Thin Liquid Films: Structure and Dynamics Studied with Coherent X Rays. *Phys. Rev. Lett.* **2007**, 99 (9).

(59) Swartjes, J. J.; Veeregowda, D. H.; van der Mei, H. C.; Busscher, H. J.; Sharma, P. K. Normally Oriented Adhesion versus Friction Forces in Bacterial Adhesion to Polymer-Brush Functionalized Surfaces Under Fluid Flow. *Adv. Funct. Mater.* **2014**, 24 (28), 4425–4441 DOI: 10.1002/adfm.201400217.

(60) Newby, B.; Chaudhury, M.; Brown, H. Macroscopic evidence of the effect of interfacial slippage on adhesion. *Science* **1995**, 269 (5229), 1407–1409.

(61) Nendza, M. Hazard assessment of silicone oils (polydimethylsiloxanes, PDMS) used in antifouling-/foul-release-products in the marine environment. *Mar. Pollut. Bull.* **2007**, 54 (8), 1190–1196.

(62) Ooms, G. *Fluid-mechanical studies on core-annular flow*. Doctoral dissertation, Drukkerij Demmenie en Zn. NV, 1971.

(63) Bannwart, A. c. Modeling aspects of oil-water core-annular flows. *J. Petrol. Sci. Eng.* **2001**, 32 (2), 127–143.

(64) Asiegubu, C.; Asakura, K. Experimental study on pressure loss of horizontal core-annular flow. *J. Solid Mech. Mater. Eng.* **2008**, 2 (6), 831–841.

(65) Curtis, J.; Klykken, P. A *Comparative Assessment of Three Common Catheter Materials*; Dow Corning: Midland, MI, 2008.

(66) Bondurant, S.; Ernster, V.; Herdman, R. *Safety of Silicone Breast Implants*; National Institutes of Health: Washington, D.C., 1999.

(67) Colas, A.; Curtis, J., Silicone Biomaterials: History and Chemistry. In *Biomaterials Science: An Introduction to Materials in Medicine*, 2nd ed.; Elsevier: Amsterdam, 2004; pp 80–85, 697–701.

(68) Lichter, J. A.; Thompson, M. T.; Delgadillo, M.; Nishikwa, T.; Rubner, M. F.; Van Vliet, K. J. Substrata Mechanical Stiffness Can Regulate Adhesion of Viable Bacteria. *Biomacromolecules* **2008**, 9, 1571–1578.

(69) Adams, F.; Romero, I.; Silva, C.; Manzan, R. Evaluation of silicon oil on bacterial growth. *Arq. Bras. Oftalmol.* **2012**, 75 (2), 89–91.

(70) Trautner, B. W.; Hull, R. A.; Darouiche, R. O. Prevention of catheter-associated urinary tract infection. *Curr. Opin. Infect. Dis.* **2005**, 18 (1), 37.

(71) Beiko, D. T.; Knudsen, B. E.; Watterson, J. D.; Cadieux, P. A.; Reid, G.; Denstedt, J. D. Urinary tract biomaterials. *J. Urol.* **2004**, 171 (6), 2438–2444.

(72) Saint, S.; Lipsky, B. A.; Baker, P. D.; McDonald, L. L.; Ossenkop, K. Urinary catheters: what type do men and their nurses prefer? *J. Am. Geriatr. Soc.* **1999**, 47 (12), 1453–1457.